Erratum in Physiol. Res. 51: 323, 2002
Physiol. Res. 51: 205-215, 2002

Model of Spike Propagation Reliability Along the Myelinated Axon Corrupted by Axonal Intrinsic Noise Sources

E. KURIŠČÁK, S. TROJAN, Z. WÜNSCH

Institute of Physiology, First Faculty of Medicine, Charles University, Prague, Czech Republic

Received January 23, 2001
Accepted September 6, 2001

Summary

We investigated how selected electromorphological parameters of myelinated axons influence the preservation of interspike intervals when the propagation of action potentials is corrupted by axonal intrinsic noise. Hereby we tried to determine how the intrinsic axonal noise influences the performance of axons serving as carriers for *temporal coding*. The strategy of this coding supposes that interspike intervals presented to higher order neurons would minimally be deprived of information included in interspike intervals at the axonal initial segment. Our experiments were conducted using a computer model of the myelinated axon constructed in a software environment GENESIS (GEneral NEural SImulation System). We varied the axonal diameter, myelin sheath thickness, axonal length, stimulation current and channel distribution to determine how these parameters influence the role of noise in spike propagation and hence in preserving the interspike intervals. Our results, expressed as the standard deviation of spike travel times, showed that by stimulating the axons with regular rectangular pulses the interspike intervals were preserved with microsecond accuracy. Stimulating the axons with pulses imitating postsynaptic currents, greater changes of interspike intervals were found, but the influence of implemented noise on the jitter of interspike intervals was approximately the same.

Key words
Axons • Action Potentials • Stochastic Processes • Computer Simulation • Ion Channels

Introduction

Axons are important structures transmitting information between neurons. Less is known about the modes by which information in neurons is represented, how it is transmitted by axons and how the properties of axons influence the capacity of transmission. Several conceptions have discussed modes of representation of information in the nervous system (NS), based mainly on the presumption that almost all information is encoded in the sequence of action potentials (AP). One of these conceptions, *rate coding*, supposes that stimuli are encoded by neurons as an average firing rate of APs (Koch 1999) and the precise occurrence of APs is only accidental and does not provide any information. This coding strategy does not require structures which reliably transmit interspike intervals. On the contrary, *temporal coding* assumes that stimuli are also encoded by neurons in the temporal pattern of APs, precise interspike intervals of which therefore represent additional information (Bialek *et al.*. 1991, Theunissen and Miller 1995, Koch 1999). In order that the information encoded by temporal coding be transmitted to the higher order neurons without significant loss of information, the axons

Fax+420 2 249 20 590
E-mail physres@biomed.cas.cz http://www.biomed.cas.cz/physiolres

should be able to transform reliably the spike pattern elicited at the axonal initial segment to the spike pattern read at postsynaptic structures. Finding the causes affecting this reliability is important for determining the extent to which axons support temporal coding. One of the most significant axonal properties affecting the interspike interval is that the APs of the actual spike pattern, due to membrane refractoriness by previous APs, propagate at different conduction velocities (George 1977, Moradmand and Goldfinger 1995). Thus the interspike intervals generated at the axonal initial segment are changed during propagation, but these changes are constant when the same spike pattern is repeatedly presented to the axon. Because of this, the major cause making the propagation unreliable is the noise and we therefore concentrated in our work on the following question: "W*hat is the influence of axonal intrinsic noise on the precision of AP propagation and how do some of the axonal parameters affect this role of noise"*. By the *„precision of AP propagation",* which we denote as *PP,* we understand the ability of the axon to maintain the AP propagation velocity constant and hence to conserve interspike intervals during propagation. The influence of noise on the *PP* was studied experimentally on frog sciatic nerve fibers (Lass and Abeles 1975) and also by means of computer modeling on thin nonmyelinated nerve fibers (Horikawa 1991). The results from these experiments showed that the *PP* expressed as standard deviation of the travel times of APs propagating along the axon can only be 5 μs (computed for 10 cm long fibers with a radius of several μm) by stimulating with a repeated pattern of current. However, this work did not analyse the relation between the *PP* and various electromorphological parameters of myelinated axons. Because of the latter, new possibilities in computer modeling and intensive discussions in the field of neuronal coding attracted our attention to these problems. We took advantage of computer modeling methods and performed all experiments evaluating the *PP* for axons of varying diameters, extent of myelinization, channel distribution and levels of thermal and channel noise. We chose computer simulations because it is not possible to ensure experimental conditions allowing variations of such desired parameters on real axons.

Methods

Our experimental method comprised computer modeling. Using the software environment GENESIS 2.1 (GEneral NEural SImulation System, see Bower and Beeman 1994), designed for construction and simulation of neuronal compartmental models, we constructed our own multicompartmental models of myelinated axons based on morphophysiological data (described below). The model consisted of internodium segments and segments of Ranvier nodes connected linearly, denoted as *membrane compartments* (top of Fig. 1). Each *membrane compartment* was connected with one *stochastic Na^+ channel compartment* and one *K^+ channel compartment,* the numbers of their Na^+ or K^+ channels corresponded to the channel distribution in real axons (Black e*t al.* 1990, Scholz e*t al.* 1993). Using special algorithm which we implemented in the GENESIS system (see APPENDIX for *channel noise*), the *stochastic channel compartments* simulated a conductance of an arbitrarily large number of stochastically behaving voltage-gated ionic channels distributed along the axon. The random fluctuation of the states of these channels was responsible for the *channel noise*. We also implemented into the model the *thermal noise* (for details see APPENDIX*)* by connecting the *membrane compartments* with a random number generators injecting randomly current into the membrane.

To determine the role of the noise on the *PP* by taking in consideration various mechanisms of generation of AP, we stimulated the axonal model at its beginning with rectangular current pulses of regular distribution (at a frequency 330 Hz and 300 μs of pulse duration, Fig. 1B) or with pulses imitating postsynaptic currents (Fig. 1C). The latter, $I_{syn}(t)$, were generated as the response of α-filter function $g_{syn}(t)$ (Rall 1967) to the Dirac pulses arriving at time intervals of Poisson distribution, multiplied by the difference between the electrochemical gradient E_{syn} of ions permeable to postsynaptic membrane and voltage $V(t)$ across it:

$$I_{syn}(t) = (V(t) - E_{syn}) \cdot g_{syn}(t) = (V(t) - E_{syn}) \cdot \alpha^2 T e^{-\alpha T}, \quad \text{[units of A]} \qquad (1)$$

where $\alpha=\tau_m/t_{peak}$, $T=t/\tau_m$, $\tau_m=Rm \cdot Cm$ is the membrane time constant, t is the simulation time and t_{peak} is the time-to-peak of the conductance transient.

To compare the *precision of AP propagation* (*PP*) of various axonal adjustments, we quantified this feature by the following procedure: we recorded APs using two virtual recording electrodes placed at various nodes of Ranvier, the distances from the axonal beginning of which, denoted as *s* and *e*, were varied. The time differences of occurrences of *k*-th AP at nodes of Ranvier at distances *s* and *e* were subtracted to obtain the time intervals I_k (k=1, .., m; m is the number of generated

APs during the simulation time T_{sim}), which we called the *travel times*. We used three modes of adjusting s and e positions of the recording electrodes: *modus* A (s was at the axonal beginning and e at the end), *modus* B (s was at the axonal beginning and e moved from the axonal beginning through selected nodes of Ranvier to the axonal end), *modus* C (the positions s and e of selected nodes of Ranvier were combined to obtain all their binary combinations). From all *travel times* I_k measured for particular s and e position, we evaluated the standard deviation $\sigma_{e,s}$ representing *precision of AP propagation* (*PP*), and for all (depending on used modus) combinations of positions s and e, we evaluated the set of standard deviations $\sigma_{e,s}$.

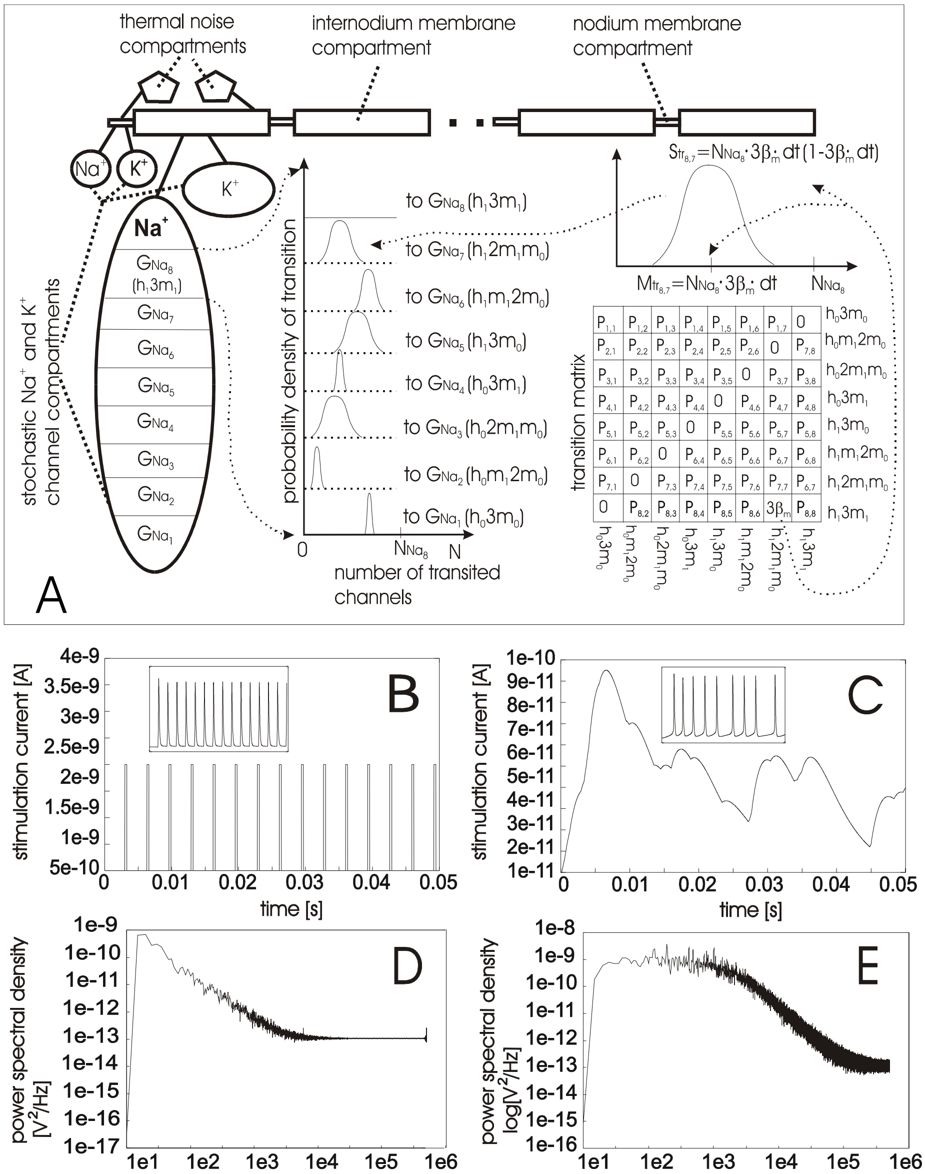

Fig. 1. *Structure and characteristic of axonal compartmental model.* ***(A)*** *Particular segments (compartments) constituting axonal model (depicted at top) and the operation of the stochastic channel compartments (e.g., for Na$^+$ channels, depicted below). Each stochastic Na$^+$ channel compartment is divided into eight groups G_{Na_i}, each containing number N_{Na_i} of channels in particular C_{Na_i} gate-configuration. Numbers N of channels transiting from, e.g. group G_{Na_8} ($h_1 3m_1$) to another of the eight groups G_{Na_j}, is determined by the eight random number generators of Gaussian distributions with means $M_{tr_{8,j}}$ and variances $S_{tr_{8,j}}$ derived from transition matrix (construction of one Gaussian is depicted at top right for the transition to G_{Na_7} ($h_1 2m_1 m_0$).* ***(B, C)*** *show modes of stimulation,* ***(B)*** *with regular rectangular current pulses and* ***(C)*** *with postsynaptic pulses. The insets represent axonal responses to both stimulations.* ***(D)*** *The power spectral density of voltage fluctuations recorded at node of Ranvier in the middle of the whole axon (1 cm in length and 3 μm in diameter) and* ***(E)*** *at separate nodal membrane. Both spectral densities are evaluated without stimulating the axon and at rest (-70 mV); the co-ordinates are in common log-log scales.*

The electromorphological parameters of our model were implemented according to available data (Tasaki 1959, Black *et al.*. 1990, Traub *et al.*. 1994, Zachary and Sejnowski 1998). Some of the parameters are listed below:

Rm_n	= 0.005	; specific nodal membrane resistance	[$\Omega \cdot m^2$]
Rm_{in}	= 10	; specific internodal membrane resistance	[$\Omega \cdot m^2$]

Cm	= 0.01	; specific membrane capacitance	[farads/m^2]
Ra	= 1.0	; specific axial resistance	[Ω·m]
Em	= -73	; membrane leakage potential	[mV]
E_{Na}	= 55	; sodium equilibrium potential	[mV]
E_K	= -71	; potassium equilibrium potential	[mV]
dt	= 0.000001	; simulation time step	[s]
ρ_{nNa}, ρ_{nK}	= 2000, 200	; density of Na^+, K^+ channel in the node of Ranvier	[μm^{-2}]
ρ_{iNa}, ρ_{iK}	= 4, 20	; density of Na^+ , K^+ channel in the internodium	[μm^{-2}]
g_{Na}, g_K	= 20, 13	; conductance of Na^+ and K^+ channels	[nS]
T_{sim}	= 0.2	; duration of simulation	[s]
l	= 1, 10	; axonal length	[cm]
d	= 0.3 - 23	; axonal diameter	[μm]
l_{in}	= 100 - 4000	; length of internodium	[μm]
l_n	= 0.3 - 10	; length of node of Ranvier	[μm]
R	= 0.003	; ratio between the l_{in} and the l_n	[1]
N_{myel}	= 3 - 210	; number of myelin membranes	[1]
V_{rest}	= -80	; membrane resting potential	[mV]
σ^2_{Ith}	= 2e^{-17} - 1e^{-13}	; variance of the current fluctuations due to thermal noise	[A^2]
T	= 309	; absolute temperature	[K]

To approach the realistic behavior of a real axon, we iterated the values of V_{rest}, dt, Ra, ρ_{nNa}, ρ_{nK}, ρ_{iNa}, ρ_{iK} and E_K, trying to adjust the features of our model (AP propagation velocity, refractoriness to stimulation, maximal frequency of APs, the width and amplitude of AP and course of the afterhyperpotential) so as to correspond to those of a real axon.

In order to determine the relationship between the *PP* and dimensions of the axon, we varied: axonal diameter *d*, number of myelin membranes N_{myel}, length of internodium l_{in} (depends on the axonal diameter: l_{in} =0.146x $10^3 \cdot d$, Tasaki 1959), length of node of Ranvier l_n. We also varied other parameters: ρ_{nNa}, ρ_{nK}, ρ_{iNa}, ρ_{iK}, E_K, N_{myel} and σ^2_{Ith} in order to assess the influence which has the number of voltage-gated channels, potassium equilibrium potential, number of myelin membranes and the power of thermal noise on the *PP*.

Results

In the first series of our simulations the axon was stimulated by regular rectangular current pulses (Fig. 1B). To determine the influence of axonal dimensions on the *PP* we varied the diameter of the axon. The relationship between the axonal diameter and the *PP* – represented by $\sigma_{s,e}$ – is depicted in Fig. 2A (for 10 cm long axons of diameter varying from 3 μm to 23 μm), and in Fig. 2B (for 1 cm long axons of diameter varying from 0.3 μm to 3 μm). Increasing axonal diameter from 0.3 μm to 23 μm decreased the value of $\sigma_{s,e}$ from 25 μs to 1 μs. The relation between the AP propagation velocity and the axonal diameter is shown in Fig. 2C and 2D (Rushton 1951, Ritchie 1982), demonstrating behaviour of our model for propagation of APs.

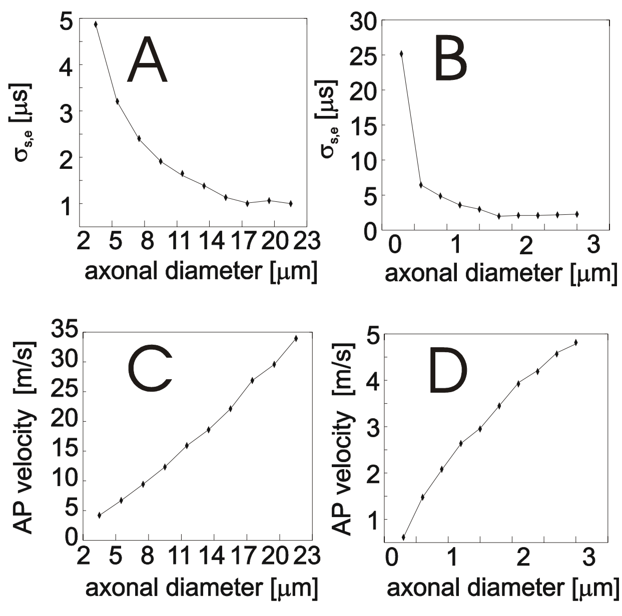

Fig. 2. *Axonal dimension and its influence on the PP and AP propagation velocity.* ***(A, B)*** *By increasing the diameter of the axon the standard deviations* $\boldsymbol{\sigma_{s,e}}$ *decreased.* ***(A)*** *shows* $\boldsymbol{\sigma_{s,e}}$ *for axons 10 cm in length, and* ***(B)*** *for axons 1 cm in length.* ***(C, D)*** *The relation between the axonal diameter and* ***AP*** *propagation velocity. All graphs are depicted in The A mode.*

In order to determine the influence of the thermal noise on the *PP,* we varied the σ^2_{Ith} variance of the current noise from $2e^{-17}$ to $1e^{-13}$ [A^2], which corresponded to the temperature change from –272 °C to 3600 °C (see Appendix equation (4)). In this case the channel noise was not implemented in the axon. The relation between the σ^2_{Ith} and $\sigma_{s,e}$ is depicted in Fig. 3A, showing smaller influence of thermal noise on the *PP* than of the channel noise, even at impracticably high temperatures. The axonal length was 1 cm and the axonal diameter 3 µm.

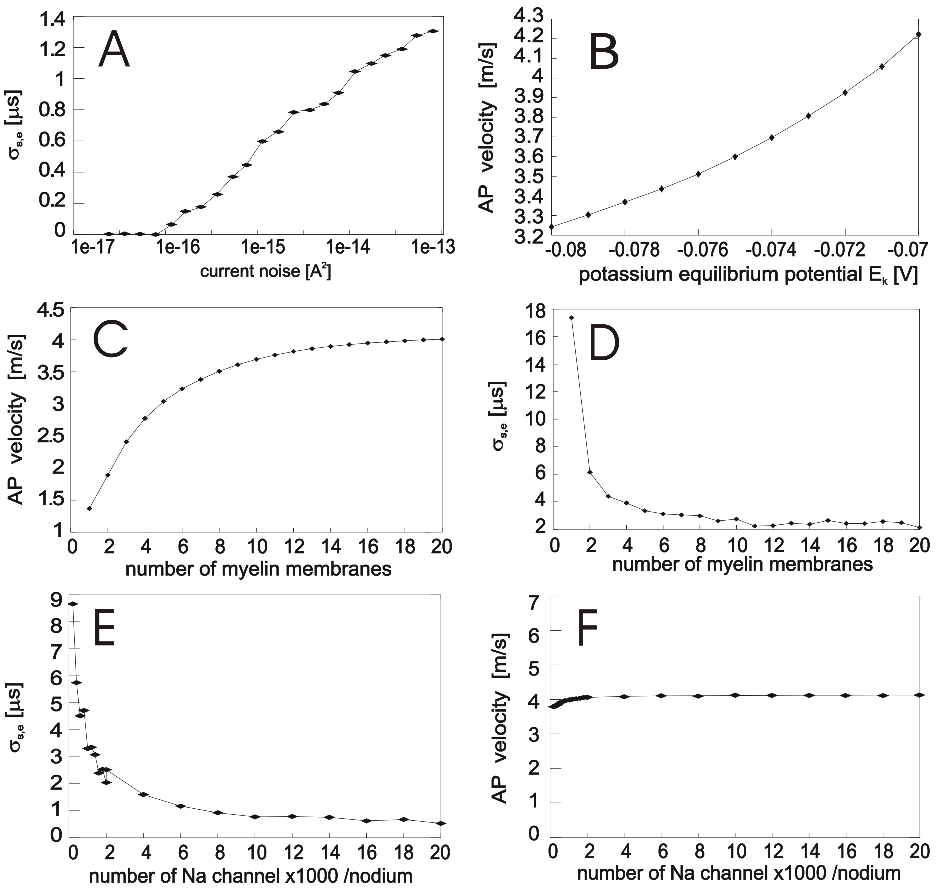

Fig. 3. *Influence of the thermal noise, myelinazation and number of channels on the PP.* ***(A)*** *By increasing the level of the thermal noise power from $2e^{-17}$ to $1e^{-13}$ [A^2] increased the values of standard deviation $\sigma_{s,e}$. The first four values of $\sigma_{s,e}$ are zero because the simulation time step dt and the number of generated* ***AP*** *were too small to enable the $\sigma_{s,e}$ to cross the non-zero value.* ***(B)*** *The influence of E_K on the* ***AP*** *propagation velocity.* ***(C)*** *Myelinization affects the AP propagation velocity and the value of $\sigma_{s,e}$* ***(D)****.* ***(E)*** *By increasing the number of voltage-dependent channels (the net conductance of each particular axonal segment was kept constant) the values of $\sigma_{s,e}$ decreased, but due to constant net conductance the propagation velocity of* ***AP*** *was affected minimally* ***(F)****. All graphs are depicted in the A mode. In all cases* ***(A-F)*** *the axonal length was 1 cm and the axonal diameter 3 µm.*

Furthermore we were interested whether the value of E_K influences the precision of AP propagation. We varied E_K from –70 mV to –80 mV and found only nonsignificant dependence between the $\sigma_{s,e}$ and the E_K. On the contrary, the value of E_K influenced the AP propagation velocity, implicating the role of E_K in the time course of the afterhyperpotential (Fig. 3B). The axonal length was 1 cm and the axonal diameter 3 µm.

In order to establish the role of myelinization for the *PP*, we varied the thickness of the myelin sheath. By increasing the number of myelin membranes, the value of $\sigma_{s,e}$ decreased reaching 2 µs without a further decrease. The largest value of $\sigma_{s,e}$ (18 µs for one myelin membrane) was ten times greater than the smallest value of $\sigma_{s,e}$ (2 µs for twenty myelin membranes). The corresponding velocities of AP propagation varied from 1.5 m/s to 4.5 m/s, also confirming the influence of myelinization on AP propagation velocity in our model. These results are depicted in Fig. 3 C-D. The axonal length was 1 cm and the axonal diameter 3 µm.

Using the following arrangement, it was possible to assess the influence of the number of voltage-gated channels on the *PP* by keeping other channel-depending features (e.g. AP propagation velocity, Fig. 3F) minimally affected. We increased the number of channels by decreasing their conductances so that the net Na^+ and K^+ conductances of *Na^+ and K^+ channel compartments* remained constant („number of channels“ multiplied by “conductance” = “net conductance”). Increasing the number of Na^+ and K^+ channels a hundred times (e.g., for

ρ_{nNa} from 200 to 20000) changed the value of $\sigma_{s,e}$ from 9 µs to 1 µs (Fig. 3E). These results demonstrate the role of the stochastic fluctuations of voltage-gated channels for the *PP*. The axonal length was 1 cm and the axonal diameter 3 µm.

In Figure 4 A-D, four graphs of $\sigma_{s,e}$ are depicted for four different axonal settings. In this series of simulations, the values of $\sigma_{s,e}$ were computed by combining the positions of two recording electrodes through all binary combinations of selected *s* and *e* locations (modus C, see Methods). The values of $\sigma_{s,e}$ of the axon with channel and thermal noise are depicted in Fig. 4B. Fig. 4A shows values of the axon without channel and thermal noise, the values of the axon only with channel noise are given in Fig. 4C and the values of the axon with thermal noise are demonstrated in Fig. 4D. Fig. 4A is markedly different from Fig. 4B-D, demonstrating that the model without channel and thermal noise sources, stimulated with regular rectangular pulses, had zero values of $\sigma_{s,e}$ for all *s-e* combinations. The small values of $\sigma_{s,e}$ in Fig. 4D in comparison to those in Fig. 4B demonstrate that the influence of the thermal noise on the *PP* is smaller than of the channel noise. The small differences between the corresponding values of $\sigma_{s,e}$ in Fig. 4B and 4C introduced by the addition of thermal noise also reflect such a relationship. The quasi-parabolic shapes in Fig. 4B-D indicate the linear summations of noise variances $(\sigma_\Delta)^2$ introduced by axonal segments of lengths Δ along the axon. In this series of simulations the axonal length was 10 cm and the axonal diameter 3 µm.

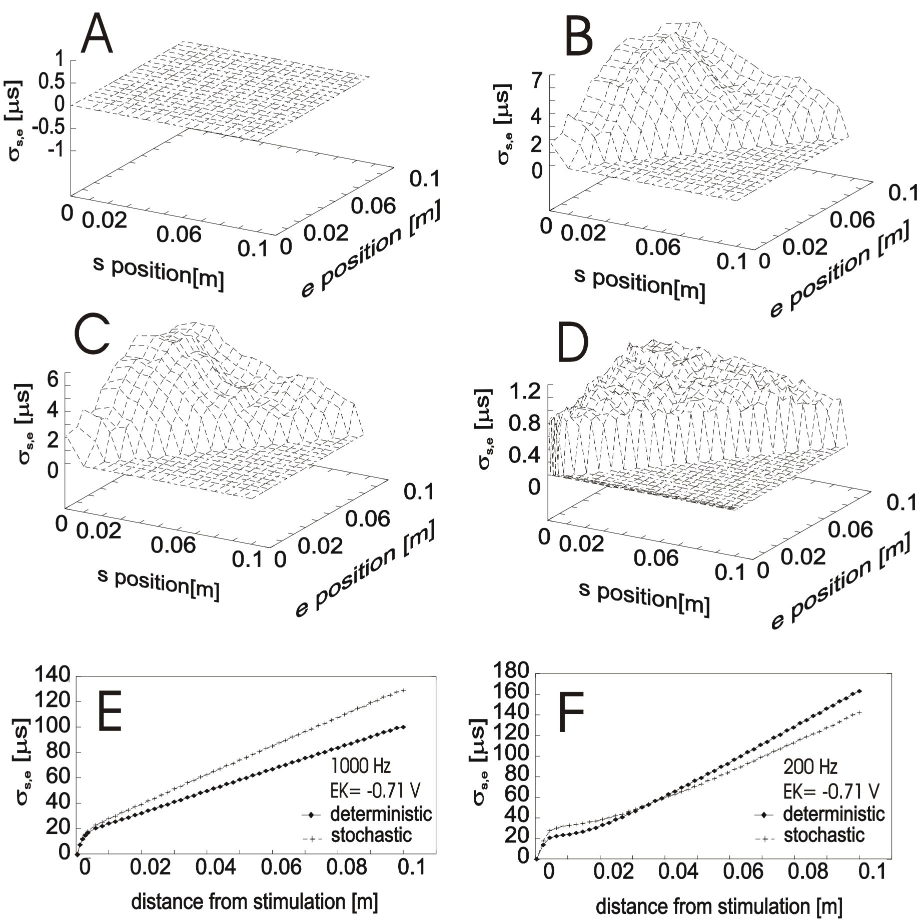

Fig. 4. *Distribution of $\sigma_{s,e}$ along the axon by stimulating with regular rectangular pulses, and the role of the noise on the PP by stimulating with postsynaptic pulses. (**A-D**) The positions of s and e electrodes are plotted on the abscissas denoted as s and e position. The values of $\sigma_{s,e}$ for correspondent s-e combinations of electrode locations are plotted on ordinate. (**A**) The $\sigma_{s,e}$ of axon without channel and thermal noise. (**B**) The $\sigma_{s,e}$ of axon with channel and thermal noise. (**C**) The $\sigma_{s,e}$ of axon with only channel noise. (**D**) The $\sigma_{s,e}$ of axon with only thermal noise. Graphs **A-D** are depicted in modus C. (**E-F**) The differences between the $\sigma_{s,e}$ of deterministic (without noise) and stochastic (with implemented channel and thermal noise) axons by stimulating with postsynaptic pulses. By this mode of stimulation the values of $\sigma_{s,e}$ were many times higher than those by stimulating with regular rectangular pulses. (**E**) The values of $\sigma_{s,e}$ by stimulating with postsynaptic pulses of frequency 1000 Hz. As the frequency of postsynaptic pulses decreased to 200 Hz, the intersection between the stochastic and deterministic curves appeared (**F**). The difference between the stochastic and deterministic $\sigma_{s,e}$ curves was of the order of $\sigma_{s,e}$ values generated by stimulating with regular rectangular pulses. Graphs (**E-F**) are depicted in the B mode. In cases (**A-F**) the axonal length was 10 cm and the axonal diameter 3 µm.*

In the previous simulation series, the axons were stimulated with regular rectangular pulses and therefore each AP had identical conditions for propagation. Such stimulation did not comply with the physiological conditions for initiating APs. We therefore stimulated the axon with a postsynaptic-like current (Fig. 1C), which caused generation of APs of various interspike intervals. By this stimulation, the APs propagated at different velocities because of the regions of membrane made refractory by previous APs (George 1977). This altered the interspike intervals and we found greater values of $\sigma_{s,e}$ than by stimulating with regular rectangular pulses. To estimate the role of noise by this mode of stimulation, we simulated two axons; one with implemented channel and thermal noise sources (*stochastic axon*) and the other without channel and thermal noise sources (*deterministic axon*). In Fig. 4E and F we can see the differences between the *PP* of *stochastic* and *deterministic axons*. These differences indicate approximately the same influence of the noise on the *PP* as by stimulating with regular rectangular pulses. Decreasing the frequency of postsynaptic pulses, the „*stochastic*“ and „*deterministic*“ curves intersected (Fig. 3F) and it appeared possible that the implemented noise performed partial „correction“ to the interspike intervals modified by propagation.

Discussion

It was proposed by Lass and Abeles (1975) that the fundamental lower limit of interspike changes during propagation is imposed by the noise inherent in axons. Our simulation results showed that by stimulating axons (with implemented channel and thermal noise) with regular rectangular pulses, the greatest influence on the *PP* (*precision of AP propagation*) had the dimension of the axon, similarly as was shown for nonmyelinated axons reported by Horikawa (1991). Furthermore, we tried to assess the influence of parameters related to the dimension of myelinated axons on the *PP*. We therefore varied the number of voltage-gated channels and the myelin sheath thickness separately and found their significance for the *PP*. We also separated the influences of the channel and thermal noise and found that the channel noise affected the *PP* more significantly than the thermal noise. This was in contradiction to the work of Horikawa (1991), probably due to small dimension and different electromorphological properties of unmyelinated axons. These results were obtained by stimulating axons with regular rectangular pulses where the APs were generated with interspike intervals of constant lengths setting the membrane homogeneously refractory for the following APs.

However, APs are not elicited *in vivo* by regular rectangular pulses and we therefore stimulated axons with a postsynaptic-like current causing generation of interspike intervals of various lengths. Due to the latter, the membrane was made inhomogeneously refractory by previous APs causing the APs to be propagated at various velocities. This changed the interspike intervals during propagation (George 1977), which was manifested by a substantial decrease of the *PP*. The extent to which axons perform changes of interspike intervals depends on the kinetics of the voltage-gated channels used. In human myelinated axons several types of K^+ voltage-gated channels (Black *et al.*. 1990, Scholz *et al.*. 1993, Reid *et al.*. 1999) were found, the interplay of which may cause more complex modifications of interspike intervals than our model. However, when the axons were stimulated by a repeated pattern of postsynaptic-like currents, the changes were constant except for the randomness induced by implemented channel and thermal noise. This randomness was comparable to the randomness measured by stimulating with regular rectangular pulses. Therefore, we suppose that if the postsynaptic structures reading the APs pattern would have „deconvolution“ ability to reconstruct interspike intervals as they were at the initial part of axon, the interspike intervals would only be distored by the noise.

We found, that the standard deviation $\sigma_{s,e}$ of the *travel times* of APs, evaluated by stimulating with regular rectangular pulses and in the presence of both types of noise (channel and thermal noise), was about 5 μs for the 10 cm long and 3 μm thick myelinated axons. These values endow axons with the performance which, if the axons indeed perform „deconvolution“, could support temporal coding with a precision within μs. However, the question remains whether the neurons are able to produce the spike pattern with such precision related to time-varying stimuli (Mainen and Sejnowski 1995, Reich e*t al.* 1997, Oram *et al.* 1999). In most neuronal systems, interspike variation of few microseconds introduced by axons does not probably disturb the information encoded in the spike pattern, but in some cases, e.g. in the auditory system, an extremely sensitive timing mechanism detecting interaural time differences of 10 μs (Moiseff and Konishi 1981), based on coincidence detection, requires axons preserving interspike intervals at the corresponding time level. It is supposed that the coincidence detection is also occurring in many cortical neurons (Konig e*t al.* 1996), thus highlighting the possible role of axonal intrinsic noise for the limitation of transmission of information from the lower order to the higher order neurons.

Although the axonal propagation may be affected by other additional sources of noise, e.g. firing of adjacent axons, potentials of neighboring synapses, diffusion of electrolytes etc., we did not consider these noises because of the methodical difficulties and absence of necessary data. However, our simulation results are in good agreement with experimental data, where the additional noises were present (*e.g.* Lass and Abeles 1975). Therefore, we assume that the same sources of noise as we implemented in our model are mainly responsible for the jitter of interspike intervals in real axons.

Appendix

Channel noise

Each Na^+ and K^+ voltage-gated ionic channel consists of subunits (gates), which behave like binary switches. The Na^+ channel consists of three activating *m*-gates and one inactivating *h*-gate, while the K^+ channel has four activating *n*-gates. Briefly, each gate may be in an open or closed state, transiting stochastically and without memory between them (the Markov process, see Kristak 1998):

$$G_0 \underset{\beta}{\overset{\alpha}{\longleftrightarrow}} G_1 , \qquad (2)$$

where G_1 denotes the open (i.e. not inactivated) gate and G_0 the closed (i.e. inactivated) gate, α and β are the voltage-dependent rate constants (3). We suppose that the transitions of gates in a particular channel are mutually independent. According to the immediate combinations of the gates, each voltage-gated channel may be in eight (for the Na^+ channel: h_03m_0, $h_0m_12m_0$, $h_02m_1m_0$, h_03m_1, h_13m_0, $h_1m_12m_0$, $h_12m_1m_0$, h_13m_1; denoted also as CNa_i, i=1, .., 8) or in five (for the K^+ channel: $4n_0$, $3n_0n_1$, $2n_02n_1$, n_03n_1, $4n_1$, also denoted as CK_i, i=1, .., 5) possible configurations, transiting stochastically from one configuration into another. The probabilities $p_{i,j}$ of all transitions during the simulation time step *dt* may be assigned to 8x8 (i,j=1, .., 8 for the Na^+ channel) or 5x5 (i,j=1, .., 5 for the K^+ channel) symmetric *transition matrix* (for Na^+ channel depicted in Fig. 1A at bottom right). For all *stochastic Na^+ and K^+ channel compartments* at each simulation time step, we calculated the *transition matrices*, items of which were derived from the rate constants α_m, β_m, α_h, β_h, α_n, β_n (3).

The kinetics of the Na^+ and K^+ channels in our model were set according to the kinetics of channels used by Traub *et al.* (1994):

Na activation (m): (3)

$\alpha_m=0.8\cdot(17.2-V_{rest})/(\exp((17.2-V_{rest})/4)-1)$

$\beta_m = 0.7\cdot(V_{rest}-42.2)/(\exp((V_{rest}-42.2)/5)-1)$

Na inactivation (h):

$\alpha_h = 0.32\cdot\exp((42.0-V_{rest})/18)$

$\beta_h = 10/(1+\exp((42.0-V_{rest})/5))$

K activation (n):

$\alpha_n=0.03\cdot(17.2-V_{rest})/(\exp((17.2-V_{rest})/5)-1)$

$\beta_n = 0.45\cdot\exp((12-V_{rest})/40)$

[units in ms^{-1}]

The kinetics of these channels was several times faster than those of the classic Huxley-Hodgkin channels (Hodgkin and Huxley 1952).

In each nodal or internodal *stochastic channel compartment*, there were on the average several thousands voltage-gated ionic channels. Depending on the actual gate-configuration of these channels, the Na^+ or K^+ channels in the *stochastic channel compartment* were distributed into eight GNa_i (for the Na^+ channel, see Fig. 1A) or five GK_i (for the K^+ channel) groups, each group containing the number NNa_i or NK_i of channels being in the CNa_i or CK_i gate-configuration. The probability of transition of the defined number of channels from one group to another during the time step *dt* is determined by the binomial distribution (DeFelice 1981b). If the number of channels in the *stochastic channel compartment* is large enough, which occurred in our case, the Gaussian distribution of defined variance Str and mean Mtr approximates the binomial distribution. To generate a new distribution of channels in the *stochastic channel compartment* at each simulation time step, we derived from the *transition matrix* the means $Mtr_{i,j}=NNa_i{\cdot}p_{i,j}$ and the variances $Str_{i,j}= NNa_i \cdot p_{i,j}{\cdot}(1-p_{i,j})$ of 64 (for Na^+ channels) or of 25 (for K^+ channels) different Gaussian distributions. For example, one Gaussian distribution for the transition from GNa_8 (h_13m_1) to GNa_7 ($h_12m_1m_0$) is depicted in Fig. 1A (at top right). The outputs from a random number generators of the mentioned Gaussian distributions were the numbers N of channels transiting between groups within the *stochastic channel compartments*. Because only the channels in group GNa_8 (gate configuration h_13m_1) or in GK_5 (gate configuration

$4n_1$) were open, the fluctuation of NNa_8 or NK_7 in each *stochastic channel compartment* was responsible for the *channel noise*. Using this method we simulated the *channel noise* more rapidly than it was possible by the Monte Carlo approach, with the same dynamics of voltage-dependent channels as by a numerical solution of the Huxley-Hodgkin differential equations.

Thermal noise

The thermal Johnson noise represents a fundamental inherent noise in the real systems. The effect of this noise can only be reduced by decreasing temperature or impedance (DeFelice 1981a). Thermal noise can easily be modeled because the power spectral density S_{Ith} of the current fluctuation of a resistance R is flat for all frequencies (white noise):

$$S_{Ith}(f) = 2\cdot k\cdot T/R \quad \text{[units of } A^2/Hz] \qquad (4)$$

where T is the absolute temperature of the conductor, k denotes the Boltzman constant, f is the frequency. We modeled the resultant thermal noise as an output from the random number generators connected to the *membrane compartments* of known specific nodal and internodal membrane resistances Rm_n and Rm_{in}, injecting into them random currents of Gaussian amplitude distribution with zero mean and σ^2_{Ith} variance:

$$\sigma^2_{Ith} = \int_{-B}^{+B} S_{Ith}(f)\,df = 4\cdot k\cdot T\cdot B/R \quad \text{[units of } A^2] \qquad (5)$$

$B = 1/dt$ [units of Hz] denotes the bandwidth of the measurement system, in our case the reciprocal value of the simulation time step. All generators of thermal noise were mutually independent.

We transcripted the algorithm for generation of channel and thermal noise into the C language script and incorporated it in the GENESIS simulator. We measured the power spectral densities of voltage fluctuations at the axonal membrane to verify the correctness of implementation of the channel and thermal noise. In Fig. 1D is the power spectral density at the nodal membrane of the whole axon with diameter 3 μm and of length 1 cm measured at rest. The course resembles the 1/f noise (DeFelice 1981). In Fig. 1E the power spectral density at a separate patch of nodal membrane of area 11 μm^2 resembles Lorentian noise (DeFelice 1981). These power spectral densities are comparable, considering their amplitude and course, to those measured experimentally (Siebenga e*t al.* 1972) or to those computed analytically (Manwani and Koch 1999).

Acknowledgements

This work was supported by the grant Research Project MSM 111100001. A preliminary communication (Kuriščák *et al.* 2000) was presented at the Meeting of Czech and Slovak Physiological Societies, Hradec Králové February 2-4, 2000 and (Kuriščák *et al.* 2001) was presented at the Meeting of Czech and Slovak Physiological Societies, České Budějovice, February 7-9, 2001.

References

BIALEK W, RIEKE F, VAN STEVENINCK RRD, WARLAND D: Reading a neural code. *Science* **252:** 1854-1857, 1991.

BLACK JA, KOCSIS JD, WAXMAN SG: Ion channel organization of the myelinated fiber. *Trends Neurosci* **13:** 48-54, 1990.

BOWER JM, BEEMAN D: The book of GENESIS: Exploring realistic neural models with the general neural simulation system. Telos/Springer Press, 1994.

DEFELICE LJ: Johnson noise. In: *Introduction to Membrane Noise.* DEFELICE LJ (ed), Plenum Press, New York, 1981a, pp 233-336.

DEFELICE LJ: Bernoulli‘s distribution for two independent two-state subunits. In: *Introduction to Membrane Noise.* LJ DEFELICE (ed), Plenum Press, New York, 1981b, pp 316-319.

GEORGE SA: Changes in interspike interval during propagation: quantitative description. *Biol Cybern* **26**: 209-213, 1977.

HODGKIN AL, HUXLEY AF: A quantitative description of membrane current and its application to conduction and excitation in nerve. *J Physiol Lond* **117:** 500-544, 1952.

HORIKAWA Y: Noise effects on spike propagation in the stochastic Hodgkin-Huxley models. *Biol Cybern* **66:** 19-25, 1991.

KOCH C: Rate codes, temporal coding, and all of that. In: *Biophysics of Computation: Information Processing in Single Neuron*. Koch C. (ed), Oxford University Press, New York, 1999, pp. 331-335.

KONIG P, ENGEL AK, SINGER W: Integrator or coincidence detector? The role of the cortical neuron revisited. *Trends Neurosci* **19**: 130-137, 1996.

KRISTAK M: The theoretical bases of stochastic processes (in Slovak) AX INZERT Press, Bratislava, Slovakia, 1998, pp. 11-69.

KURIŠČÁK E, TROJAN S, WÜNSCH Z: May the shape of the action potentials themselves transmit information along the myelinated axon? *Physiol Res* **50**(suppl)**:** P15, 2001.

KURIŠČÁK E, TROJAN S, WÜNSCH Z: Model of spike propagation reliability along the myelinated axon corrupted by axonal intrinsic noise sources. *Physiol Res* **49**(suppl)**:** P37, 2000.

LASS Y, ABELES M: Transmission of information by the axon: I. Noise and memory in the myelinated nerve fiber of the frog. *Biol Cybern* **19:** 61-67, 1975.

MAINEN ZF, SEJNOWSKI TJ: Reliability of spike timing in neocortical neurons. *Science* **268:** 1503-1506, 1995.

MANWANI A, KOCH C: Detecting and estimating signals in noisy cable structures: I. Neuronal noise sources. *Neural Comput* **11:** 1797-1829, 1999.

MOISEFF A, KONISHI M: Neuronal and behavioural sensitivity to binaural time differences in the owl. *J Neurosci* **1**: 40-48, 1981.

MORADMAND K, GOLDFINGER MD: Computation of long-distance propagation of impulses elicited by Poisson-process stimulation. *J Neurophysiol* **74**: 2415-2426, 1995.

ORAM MW, WIENER MC, LESTIENNE R, RICHMOND BJ: Stochastic nature of precisely timed spike patterns in visual system neuronal responses. *J Neurophysiol* **81**: 3021-3033, 1999.

RALL W: Distinguishing theoretical synaptic potentials computed for different soma-dendritic distributions of synaptic input. *J Neurophysiol* **30**:1138-1168, 1967.

REICH DS, VICTOR JD, KNIGHT BW, OZAKI T, KAPLAN E: Response variability and timing precision of neuronal spike trains in vivo. *J Neurophysiol* **77**: 2836-2841, 1997.

REID G, SCHOLZ A, BOSTOCK H, VOGEL W: Human axons contain at least five types of voltage-dependent potassium channel. *J Physiol Lond* **518**: 681-696, 1999.

RITCHIE JM: On the relation between fibre diameter and conduction velocity in myelinated nerve fibres. *Proc R So Lond B Biol Sci*. **217:** 29-35, 1982.

RUSHTON WAH: A theory of the effects of fibre size in medullated nerve. *J Physiol Lond* **115:** 101-122, 1951.

SCHOLZ A, REID G, VOGEL W, BOSTOCK H: Ion channels in human axons. *J Neurophysiol* **70:** 1274-1279, 1993.

SIEBENGA E, VERVEEN AA: Membrane noise and ion transport in the node of Ranvier. *Biomembranes* **3:** 473-482, 1972.

TASAKI I: Conduction of the nerve impulse. In: *Handbook of Physiology, section Neurophysiology, vol I.* FIELD J, MAGOUN HW, HALL VE. (eds), Waverly Press, Baltimore, Maryland, 1959, pp. 75-121.

THEUNISSEN F, MILLER JP: Temporal encoding in nervous system: a rigorous definition. *J Comput Neurosci* **2:** 149-162, 1995.

TRAUB RD, JEFFERYS GR, MILES R, WHITTINGTON MA, TOTH K: A branching dendritic model of a rodent CA3 pyramidal neurone. *J Physio Lond* **481**: 79-95, 1994.

ZACHARY F, SEJNOWSKI MTJ: Axonal structure and function. In: *Methods in Neuronal Modeling.* KOCH C, SEGEV I. (eds), The MIT Press, Cambridge, Massachusetts, London, England, 1998, pp. 190-193.

Reprint requests

E. Kuriščák, Institute of Physiology, First Faculty of Medicine, Charles University, Albertov 5, 128 00 Prague 2, Czech Republic, e-mail: ekuri@lf1.cuni.cz